Journal of Mechanical Engineering and Sciences (JMES)
e-ISSN: 2231-8380; Volume 1, pp. 37-46, December 2011

FINITE ELEMENT ANALYSIS OF HASTELLOY C-22HS IN END MILLING

K. Kadirgama, M.M. Rahman, A.R. Ismail and R.A. Bakar
Faculty of Mechanical Engineering
Universiti Malaysia Pahang
26600 Pekan, Pahang, Malaysia
Phone: +6094242355; Fax: +6094242202
Email: kumaran@ump.edu.my

ABSTRACT

This paper presents the finite element analysis to study the stress distribution of nickel based superalloy HASTELLOY C-2000 in end milling operation. A commercial finite element software was used to develop modeling and analysis the distribution of stress components in the machined surface after end milling of HASTELLOY C-22HS using coated carbide tools. The friction interaction along the tool-chip interface was modeled with Coulomb friction law. It was found that the stress had lower values under the cut surface and increased gradually near the cutting edge.

Keywords: Finite element analysis, stress, Milling

INTRODUCTION

In many industries, nickel-base alloys represent an important segment of structural materials. Critical components made of these alloys are relied upon to function satisfactorily in corrosive services. Corrosion-resistant high alloy castings are often the subject of major concern because failures of cast components have led to significant downtime costs and operating problems (Strenkowski and Carroll, 1985). Over the years, the nickel- chromium-molybdenum / tungsten alloys have proven to be among the most reliable and cost effective materials for aggressive seawater application and excellent resistance to localized corrosive attack (pitting, crevice corrosion). Among these alloys, Hestelloy C-types (C, C-4, C-276, and C-22) are used to serve the above mentioned purposes. As these alloys are commonly subject to further machining after casting, it becomes very vital to have an idea about the change in properties imparted to the machined surfaces after such cutting operations as end milling. For this reason, finite element methodology is used in this study to determine the machined surface stress characteristics.In the past decade, finite element method based on the updated-Lagrangian formulation has been developed to analyze metal cutting processes (Strenkowski and Carroll, 1985; Strenkowski and Mitchum, 1987; Shih et al., 1990). Several special finite element techniques, such as the element separation (Komvopoulos and Erpenbeek, 1991; Shih and Yang, 1993), modeling of worn cutting tool geometry (Komvopoulos and Erpenbeek, 1991; Shih and Yang, 1993; Shih, 1995), mesh rezoning (Komvopoulos and Erpenbeek, 1991; Ueda and Manabe, 1993), friction modeling (Strenkowski and Carroll, 1985; Strenkowski and Mitchum, 1987; Komvopoulos and Erpenbeek, 1991), etc. have been implemented to improve the accuracy and efficiency of the finite element modeling. Detailed work-material modeling, which includes the coupling of temperature, strain-rate, and strain hardening effects, has been applied to model material deformation (Shih et al., 1990; Shih and Yang, 1993; Shih, 1995). An early analytical model for predicting residual stresses was proposed by Okushima and

Kakino (1971), in which residual stresses were related to the cutting force and temperature distribution during machining. In another analytical model a relation was made between residual stresses and the hardness of the workpiece (Wu and Matsumoto, 1990). Shih and Yang (1993) conducted a combined experimental/computational study of the distribution of residual stresses in a machined workpiece. Liu and Guo (2000) used the finite element method to evaluate residual stresses in a workpiece. They also observed that the magnitude of residual stress reduces when a second cut is made on the cut surface. Liu and Barash (1982) measured the residual stress on the workpiece subsurface with consideration of tool flank wear. Their findings indicated that under the condition of a lower cutting speed, the mechanical load had a greater impact on residual stress, while the thermal effect become the major factor affecting residual stress at higher cutting speed. Lee and Shaffer (1951) proposed a shear-angle model based on the slip-line field theory, which assumes a rigid-perfectly plastic material behavior and a straight shear plane. Kudo (1965) modified the slip-line model by introducing a curved shear plane to account for the controlled contact between the curved chip and straight tool face. Henriksen (1951) conducted a series of tests to understand residual stresses in the machined surface of steel and cast iron parts under various cutting conditions. Kono et al. (1980) and Tonsoff et al. (1995) revealed that residual stresses are dependent on the cutting speed. Matsumoto et al. (1986) and Wu and Matsumoto (1990) observed that the hardness of the workpiece material has a significant influence on the residual stress field. Konig et al. (1993) showed that friction in metal cutting also contributes to the formation of residual stresses.

FINITE ELEMENT MODEL

The finite element model is composed of a deformable workpiece and a rigid tool. The tool penetrates through the workpiece at a constant speed and constant feed rate. The model assumes plane-strain condition since generally depth of cut is much greater than feed rate. The finite model used in this study is based on the commercial finite element software. The software, called “Thirdwave AdvantEdge” uses six-noded quadratic triangular elements by default. AdvantEdge is an automated program and it is enough to input process parameters to make a two-dimensional simulation of orthogonal cutting operation. Thermal boundary conditions for Thirdwave AdvantEdge are given as:

1. The heat is generated due to heavy plastic work done on the workpiece. Its formula is given in Eq. (1):

$$R = \frac{m \cdot f \cdot W^P}{\rho} \tag{1}$$

where W^P is the rate of plastic work, f is the fraction of plastic work converted into heat (assumed to be 0.9), m is the mechanical equivalent of heat (taken as 1) and ρ is the density of workpiece material (8.6 g/cm^3)

2. The heat is generated due to friction between the chip and the rake face of the tool according to Eq. (2).

$$q = F_{fr} \cdot V_r \cdot m \tag{2}$$

where F_{fr} is the friction force, V_r is the relative sliding velocity between tool and chip and m is the mechanical equivalent of heat (m = 1)

3. The generated frictional heat is distributed to chip and tool according to Eq. (3):

$$\frac{Q_{chip}}{Q_{tool}} = \frac{\sqrt{k_{chip} \cdot \rho_{chip} \cdot c_{chip}}}{\sqrt{k_{tool} \cdot \rho_{tool} \cdot c_{too}l}} \tag{3}$$

where Q_{chip} is the heat given to the chip, Q_{tool} is the heat given to the tool, k is the conductivity, ρ is the density and c is the heat capacity.

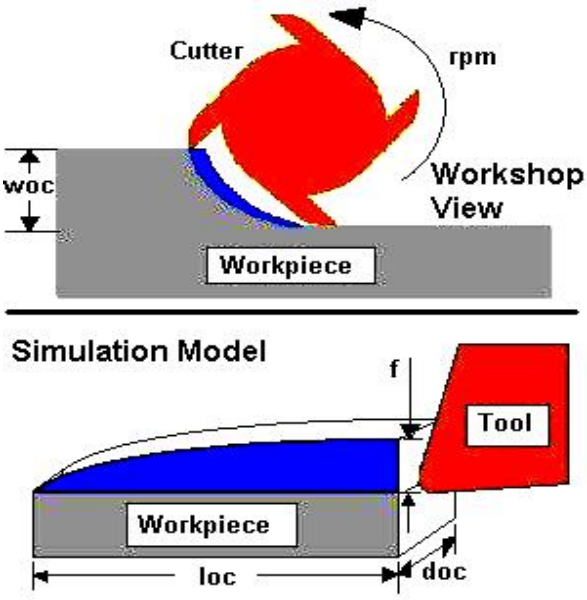

Figure 1. Model for milling.

Certain assumptions are made to simulate the complex procedure of metal cutting with FEM. These assumptions are used to define the problem to be solved as well as to apply the boundary and loading conditions:

1. The cutting speed is constant.
2. The width of cut is larger than the feed (plane strain condition), and both are constant.
3. The cutting velocity vector is normal to the cutting edge.
4. The workpiece material is a homogeneous polycrystalline, isotropic, and incompressible solid.
5. The workpiece is set at a reference temperature of 20° C at the beginning of simulation.
6. The machine tool is perfectly rigid and no influence of machine tool dynamics on machining is considered.
7. Constant friction at tool-chip interaction and tool-workpiece interaction.

Figure 1 shows the Thirdwave AdvantEdge model for milling operation and Figure 2 shows an example of visual simulation of residual stresses induced after milling.

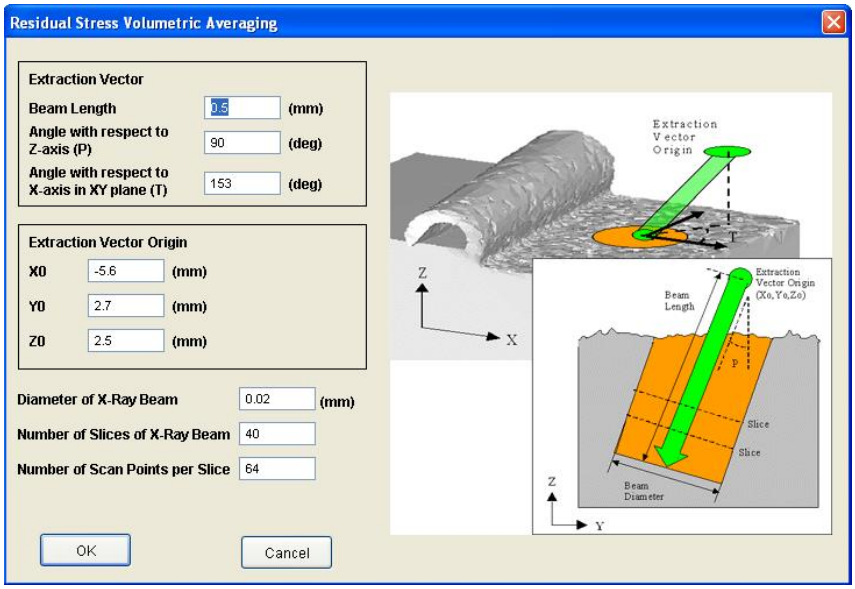

Figure 2. Model for residual stress

WORKPIECE AND TOOL MATERIAL MODELING

The workpiece material used for simulation is HASTELLOY C-22HS and the cutting tool is carbide coated with TiALN and 20° rake angle. Every one pass (80mm), the simulation was stopped. AdvantEdge uses an analytical formulation for material modeling. In a typical machining event, in the primary and secondary shear zones very high strain rates are achieved, while the remainder of the workpiece deforms at moderate or low strain rates. In order to account for this, Thirdwave AdvantEdge incorporates a stepwise variation of the rate sensitivity exponent:

$$\bar{\sigma} = \sigma_f\left(\varepsilon^p\right)\cdot\left(1+\frac{\dot{\varepsilon}^p}{\dot{\varepsilon}_o^p}\right)^{1/m_1}, \; if \;\; \dot{\varepsilon} \le \dot{\varepsilon}_t^p \tag{4}$$

where $\bar{\sigma}$ is the effective von Mises stress, σ_f is the flow stress, ε^p is the accumulated plastic strain, $\dot{\varepsilon}_o^p$ is a reference plastic strain rate, m_1 is the strain-rate sensitivity exponents, and $\dot{\varepsilon}_t$ is the threshold strain rate which separates the two regimes. In calculations, a local Newton – Raphson iteration is used to compute $\dot{\varepsilon}_o^p$ according to the low – rate equation, and switches to the high rate equation if the result lies above $\dot{\varepsilon}_t$. σ_f, which is used in Eq. (5) is given as:

$$\sigma_f = \sigma_0 \cdot \psi(T)\cdot\left(1+\frac{\varepsilon^p}{\varepsilon_0^p}\right)^{1/n} \tag{2}$$

where T is the current temperature, σ_0 is the initial yield stress at the reference temperature T_0, ε_0^p is the reference plastic strain, n is the hardening exponent and $\psi(T)$ is the thermal softening factor. In the present study, it is assumed that the tool is not plastifying. Hence, it is considered as an absolutely rigid body

Workpiece Material

The properties of the workpiece material (Hastelloy C-22HS) are shown in Tables 1 and 2. Meanwhile cutting tool properties and simulation are shown in Table 3 and 4.

Table 1. Chemical composition for Hastelloy C-22HS.

Ni	Cr	Mo	Fe	Co	W	Mn	Al	Si	C	B
BAL (%)	21	17	2	1	1	0.80	0.50	0.08	0.01	0.01

Table 2. Physical properties of Hastelloy C-22HS at room temperature.

Properties	Value
Density (g/cm^3)	8.6
Thermal Conductivity (W/m.^{o}C)	11.8
Mean Coefficient of Thermal Expansion (μm/m.^{o}C)	11.6
Thermal Diffusivity (cm^2/s)	0.0334
Specific Heat (J/kg.^{o}C)	412
Young Modulus (GPa)	223

Table 3. Cutting tool properties

Code name	**Composition (%)**						**Coating**	**Thickness (μm)**
	% Co	% WC	%Cr3C2	%TaC	%TiC	%Nbc		
KC520M	6	93.5	0.5	-	-	-	PVD TiAlN	3.5

Table 4. Simulation conditions

Simulation No.	**Cutting speed**	**Feedrate**	**Axial depth**
1	140	0.1	2
2	140	0.2	1
3	100	0.15	1
4	100	0.15	2
5	140	0.15	1.5
6	100	0.1	1.5
7	180	0.1	1.5
8	180	0.15	2
9	180	0.2	1.5
10	140	0.2	2
11	180	0.15	1
12	140	0.15	1.5
13	140	0.1	1
14	100	0.2	1.5
15	140	0.15	1.5

RESULTS AND DISCUSSION

von Mises stress, σ_V, is used to estimate yield criteria for ductile materials. It is calculated by combining stresses in two or three dimensions, with the result compared to the tensile strength of the material loaded in one dimension. Von Mises stress is also useful for calculating the fatigue strength (Schey, 2000).

Von Mises stress in three dimensions is expressed as (Schey, 2000):

$$\sigma_V = \sqrt{\frac{(\sigma_1 - \sigma_2)^2 + (\sigma_2 - \sigma_3)^2 + (\sigma_3 - \sigma_1)^2}{2}} \tag{3}$$

where $\sigma_1, \sigma_2, \sigma_3$ are the principal stresses. Figure 3 shows the von Mises stress for simulation no.9 (Cutting speed 180 m/min, feedrate 0.15 mm and axial depth 2.0 mm) after 80 mm. Most of the tensile σ_V appear at the cutting tool edge. Based on Von Mises criterion, it states that failure occurs when the energy of distortion reaches the same energy for yield/failure in uniaxial tension. Mathematically, this is expressed as (Schey, 2000),

$$\frac{1}{2}\left[(\sigma_1 - \sigma_2)^2 + (\sigma_2 - \sigma_3)^2 + (\sigma_3 - \sigma_1)^2\right] \leq \sigma_y^2 \tag{4}$$

The yield strength and ultimate tensile strength for the coated carbide cutting tool used in this simulation are 600 MPa and 800 MPa respectively. Then von Mises stress at at region 9 is 4488 MPa, which is higher than the yield strength and ultimate tensile strength of the coated cutting tool. This strees can cause permanent damage to the cutting tool since this stress is beyond the ultimate tensile strength and yield strength. Cutting speed, feedrate, and axial depth for this simulation is very high and this cause the high stress at the cutting edge, since high cutting speed, feedrate, and axial depth can cause high force in milling (Kadirgama and Abou-El-Hossein, 2005; Alauddin et al., 1998). The radial depth for every simulation is 3.5 mm. This factor also contributes to higher stress. At region 1, at the cutting tool and chip contact, the von Mises stress is 501 MPa, where the yield strength and ultimate strength of the workpiece are 359 MPa and 759 MPa. The workpiece start to deform since the stress is above its yield strength.

Figure 4 shows von Mises stress for simulation no. 3 (Cutting speed 100 m/min, feedrate 0.2 mm/rev, axial depth 1.5 mm). The stress at cutting tool edge (region 5) is 1345 MPa. The Von mises stress is lower compared to that in simulation run no. 9. Even though the stress still higher than yield strength and ultimate tensile strength, but the damage should be not severe compared to that of simulation no.9. At region 3, the stress for the contact point cutting tool and chip is 577 MPa. This value is almost the same as in simulation no.9. From the von Mises stress distribution as shown in Figure 3 and 4, most of the tensile σ_V locate at the edge of the cutting tool. The stress distribution also show the stress is lower at under the cut surface and increases gradually near the cutting edge. High force is needed at the tool edge for workpiece penetration, and this is indirectly increase the stress at the tool edge. This distribution of the stress is same for both cases. The velocity vectors for simulation no.9 as shown in Figure 5 around the tool tip, clearly show the plastic flow of the material araound the cutting

edge. The same trend of flow also was observed by Movahhedy et al., 2000). Figure 6 shows the 3D picture for von Misses stress distribution for simulation no.9. Table 3 show the average value von Mises stress at cutting tool edge for every simulation that already run. This value will be investigated through statistical method to find the relationship between variables (cutting speed, feedrate and axial depth) with response (von mises Stress).

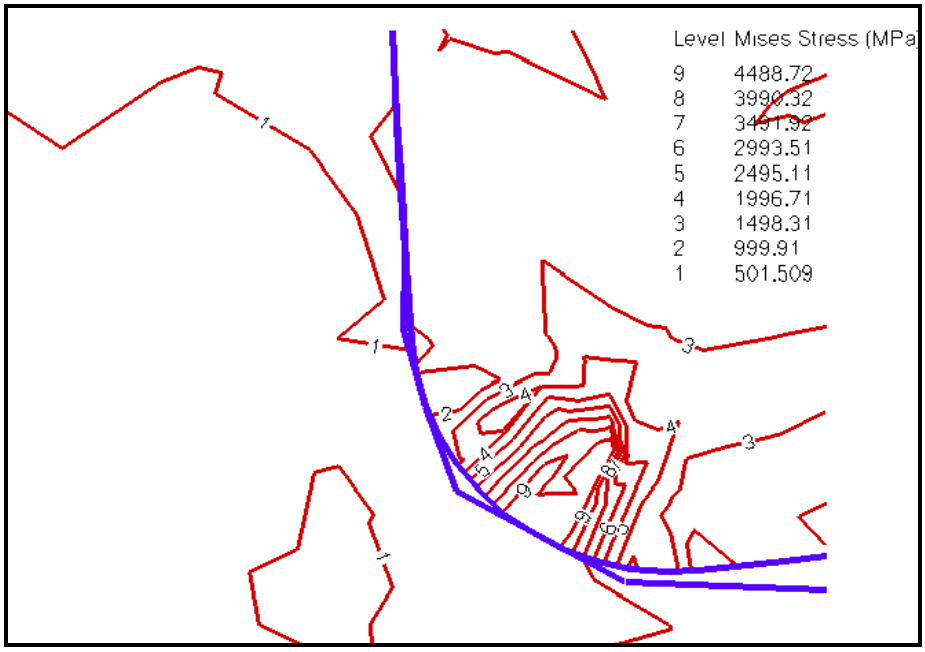

Figure 3. Von mises stress for simulation no. 9

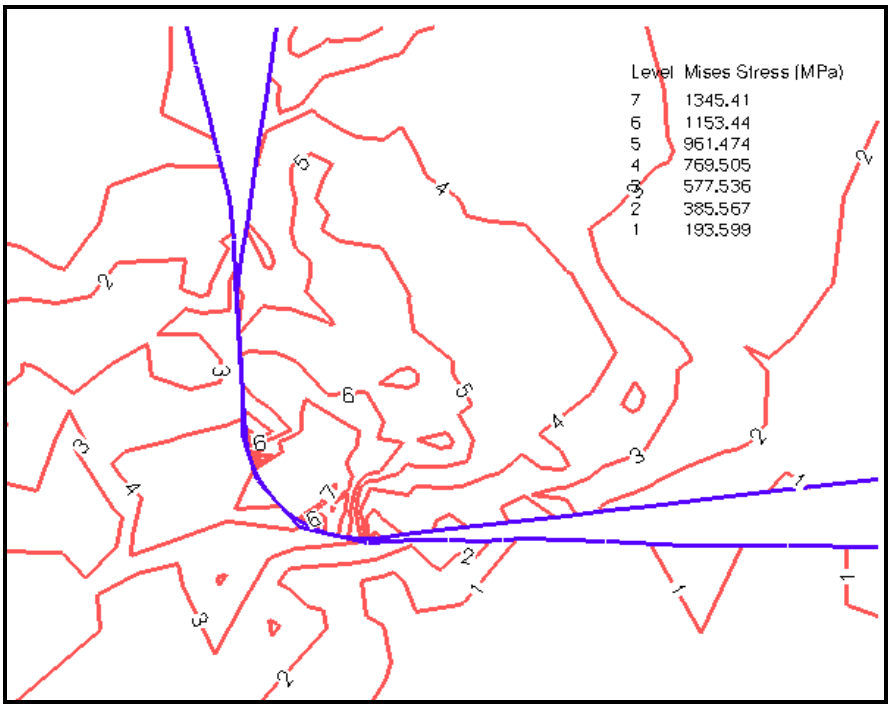

Figure 4. von Mises stress for simulation no. 3

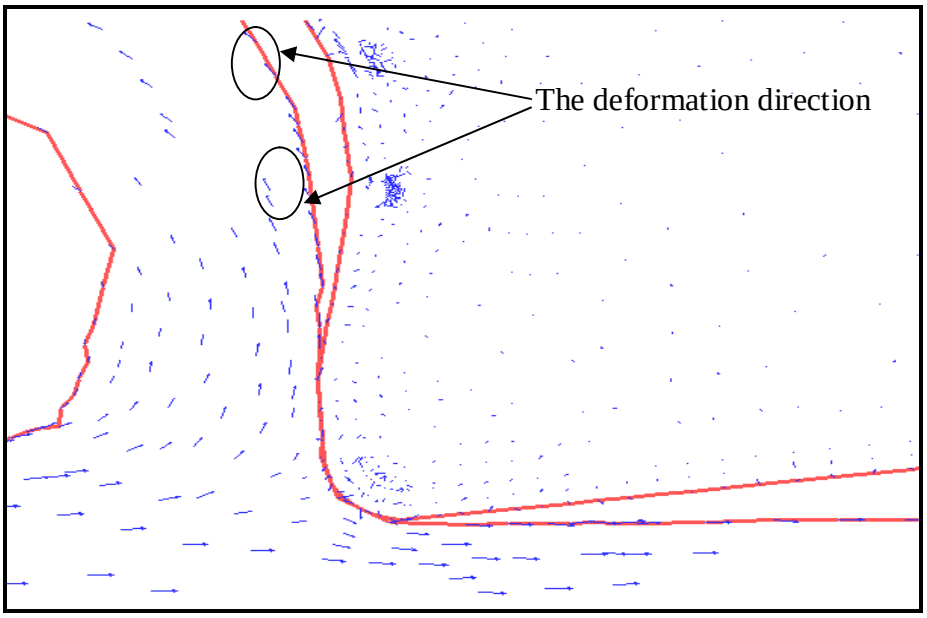

Figure 5. The velocity vectors for simulation no.9.

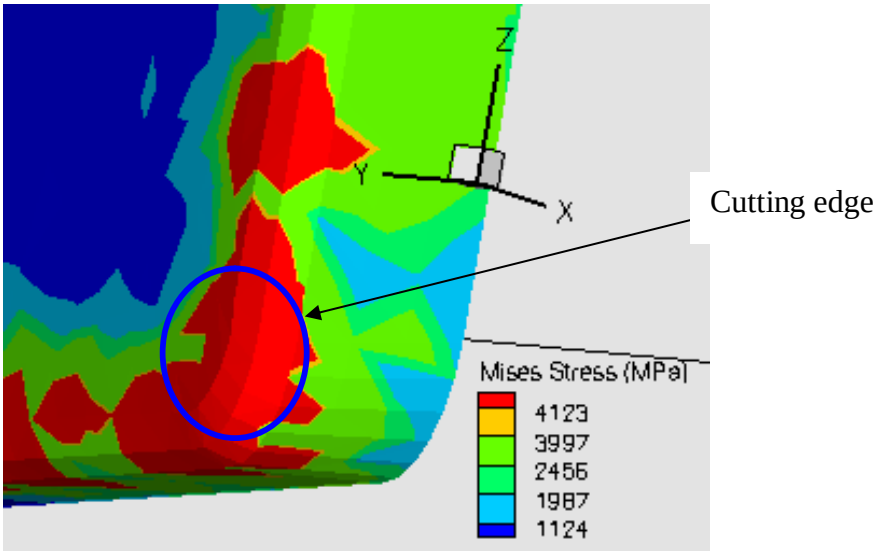

Figure 6. 3D picture for Von Misses stress distribution for simulation no. 9

CONCLUSION

In the milling operation, cutting speed, feedrate and axial depth play the major role in producing high stresses. The Von Mises stress distribution also show the stress is lower at under the cut surface and increase gradually when come at cutting edge. The highest compressive σ_{xx} appear at the cutting edge. Most of the tensile σ_V appear at the cutting tool edge. The stress distribution also show the stress is lower at under the cut surface and increases gradually near the cutting edge. High force is needed at the tool edge for workpiece penetration, and this is indirectly increasing the stress at the tool edge. This distribution of the stress is same for both cases.

REFERENCES

Alauddin, M., Mazid, M.A., EL Baradi, M.A. and M.S.J.Hashmi,"Cutting forces in the end milling of Inconel 718. Journal of Materials Processing Technology",77(1998),pp 153-159.

Henriksen, E.K. 1951. Residual stresses in machined surfaces. Transactions ASME Journal of Engineering for Industry, 73: 69–76.

Kadirgama, K., Abou-El-Hossein, K.A. 2005. Force Prediction Model for Milling 618 tool Steel Using Response Surface Methodology. American Journal of Applied Sciences, 2(8): 1222-1227.

Komvopoulos, K. and Erpenbeek, S.A. 1991. Finite Element Modelling of orthogonal cutting, *ASME 1. Engng Ind.* 113: 253.

Konig, W., Berktold, A. and Koch, K.F. 1993. Turning versus grinding—a comparison of surface integrity aspects and attainable accuracy. Annals of the CIRP, 42(1): 39–43.

Kono, Y., Hara, A., Yazu, S., Uchida, T. and Mori, Y. 1980. Cutting performance of sintered CBN tools, Cutting tool materials. Proceedings of the International Conference, American Society for Metals, Ft. Mitchell, KY, pp. 218-95.

Kudo, H. 1965. Some new slip-line solutions for two-dimensional steady state machining, International Journal of Mechanical Science 7: 43–55.

Lee, E.H. and Shaffer, B.W. 1951. The theory of plasticity applied to a problem of machining, Journal of Applied Mechanics, 18: 405–413.

Liu, C.R. and Barash, M.M. 1982. Variables governing patterns of mechanical residual stress in a machined surface. Transactions of the ASME, Journal of Engineering for Industry, 104: 257–264.

Liu, R. and Guo, Y.B. 2000. Finite element analysis of the effect of sequential cuts and tool-chip friction on residual stresses in a machined layer, International Journal of Mechanical Sciences, 42: 1069–1086.

Matsumoto, Y., Barash, M.M. and Liu, C.R. 1986. Effects of hardness on the surface integrity of AISI 4340 steel. Transactions of the ASME, Journal of Engineering for Industry, 108: 169–175.

Movahhedy, M., Gadala, M.S. and Altintas, Y. 2000. Simulation of the orthogonal metal cutting process using an arbitrary Lagrangian- Eulerian finite –element method. Journal of Materials Processing Technology,103: 267-275.

Okushima, K. and Kakino, Y. 1971. The residual stresses produced by metal cutting, Annals of the CIRP, 10(1): 13–14.

Schey, J. A. 2000. Introduction to Manufacturing Processes. McGraw Hill, 3rd ed.

Shih, A.J. 1995. Finite Element Simulation of Orthogonal Metal Cutting, *ASME 1. Engng Ind.* 117: 84.

Shih, A.J. and Yang, H.T. 1993. Experimental and finite element predictions of residual stresses due to orthogonal metal cutting. *Int. I. Numer. Meth. Engng.* 36, 1487.

Shih, J. and Yang, H.T.Y. 1993. Experimental and finite element predictions of the residual stresses due to orthogonal metal cutting, International Journal for Numerical Methods in Engineering, 36: 1487–1507.

Shih,A.J., Chandrasekar, S. and Yang, H.T. 1990. Fundamental issues in machining, ASME PED, 43: 11.

Strenkowski, J.S. and J. T. Carroll, J.T. 1985. A Finite Element Model of Orthogonal Metal Cutting, ASME 1. Eng. Ind. 107: 345.

Strenkowski, J.S. and Mitchum, G.L.1987. Proc. North American Manufacturing Conf., pp. 506.

Tonshoff, H.K., Wobker, H.G.and Brandt, D. 1995. Tribological aspects of hard turning with ceramic tools. Journal of the Society of Tribologists and Lubrication Engineers, 51: 163–168.

Ueda, K. and Manabe, K. 1993. Rigid-plastic FEM analysis of three-dimensional deformation fiels in chip formation process *Ann. CIRP* 42, 35.

Wu, D.W. and Matsumoto, Y. 1990. The effect of hardness on residual stresses in orthogonal machining of AISI 4340 steel. Transactions of the ASME, Journal of Engineering for Industry, 112: 245–252.

Wu, D.W. and Matsumoto, Y. 1990. The effect of hardness on residual stresses in orthogonal machining of AISI 4340 steel. Transactions of the ASME, Journal of Engineering for Industry, 112: 245–252.